

Measurement of density variations in tablets using X-ray computed tomography

I.C. Sinka^{a,*}, S.F. Burch^b, J.H. Tweed^b, J.C. Cunningham^c

^a Merck Sharp and Dohme Ltd., Hoddesdon, Hertfordshire EN11 9BU, UK

^b AEA Technology Plc, Culham Science Centre, Abingdon, Oxfordshire OX14 3ED, UK

^c Merck and Co., Inc., West Point, PA 19486, USA

Received 18 August 2003; received in revised form 6 November 2003; accepted 12 November 2003

Abstract

In this paper the application of X-ray computed tomography (CT) to measure the material density distribution in pharmaceutical tablets is discussed. X-ray CT is a non-destructive inspection technique which provides cross-sectional images in different planes through a component. The CT image values provide information on the local X-ray attenuation coefficients. For a particular material and X-ray energy, X-ray attenuation is approximately proportional to material density. Determination of quantitative density distributions requires consideration of non-linear instrumental effects including scatter and “beam hardening”. Density maps in tablets manufactured under controlled conditions are presented. The results are discussed with reference to the local properties of the material within the tablet and the tablet design features.

© 2003 Elsevier B.V. All rights reserved.

Keywords: X-ray computed tomography; Density distribution; Tablet

1. Introduction

Die compaction is a unit operation employed in pharmaceuticals, powder metallurgy, ceramics and other industries. During compaction complex movements take place within the powder bed and interactions occur between the powder and tooling, i.e. die wall and punch faces. As a result density variations are induced in the volume of the compact, which may affect its physical and mechanical properties.

Density measurements in powder compacts have been carried out since the early 1900s as described by Train (Train, 1957) and included techniques based

on differential machining, hardness tests or X-ray shadow of lead grids placed in the compact. Macleod and Marshall (1977) have presented autoradiography experiments using ceramic compacts possessing natural radioactivity and the density distribution patterns were discussed in the context of die wall friction. More modern techniques available to characterise compact microstructure were summarised by Lannutti (1997) and include: X-ray CT, acoustic wave velocity measurements and nuclear magnetic resonance imaging. X-ray CT has been applied to characterise density distributions in powder compacts in various fields (Lannutti, 1997; Lin and Miller, 2000, 2001; Kong and Lannutti, 2000; Burch, 2001a; Li et al., 2002; Nielsen et al., 2003).

Density variations in pharmaceutical tablets are inherent to the manufacturing process and are important

* Corresponding author. Tel.: +44-1992-452321;

fax: +44-1992-460078.

E-mail address: csaba.sinka@merck.com (I.C. Sinka).

because they may lead to differences in local properties, such as dissolution or mechanical response during post-compaction operations, packaging, storage and use.

The density distribution in tablets has been examined using surface hardness tests carried out on cross-sections of the tablets (Sinka et al., 2003). However, this destructive technique requires careful specimen preparation due to the brittle nature of the tablet. In addition, the resolution is limited by a minimum spacing requirement between indentations. X-ray CT, which is non-destructive and requires no specimen preparation, is therefore well suited for such materials. The porosity and morphology of granules (Farber et al., 2003) and preliminary assessments of the structure of tablets (Sinka et al., 2002) were reported. However, quantitative X-ray CT results for density distribution in powder compacts of size, shape and materials characteristic to pharmaceutical tablets have not yet been presented in the literature to the authors' knowledge.

The main objective of this paper is to develop a methodology for generating quantitative density maps for pharmaceutical tablets. The particular features of X-ray CT data analysis are discussed for this class of powder compacts. The density distribution in model tablets manufactured under controlled conditions is discussed in detail with respect to the consequences for formulation design, process development and tablet image design.

2. X-ray CT method

X-ray CT is a non-destructive inspection technique which provides cross-sectional images in planes through a component (Kak, 1979). The principle of third generation CT imaging, as used in the industrial context, is illustrated in Fig. 1. The component is placed on a precision turntable in the divergent beam of X-rays generated by an industrial X-ray source. A detector array (line or area array) is used to measure the intensities of the X-ray beam transmitted through the component, as the component is rotated in the beam. A mathematical algorithm (Mersereau, 1974) is then used to generate (or "reconstruct") the CT images from the measured transmitted intensities.

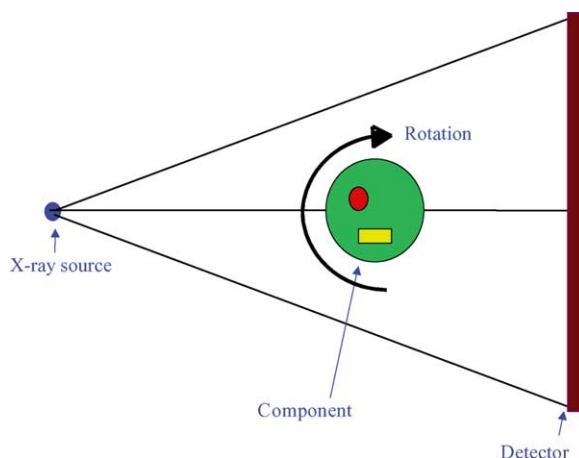


Fig. 1. X-ray CT principle.

The resultant CT images are true cross-sectional images, and show the geometry of the component in the plane of the cross-section. If an X-ray source with a small size (micro-focus source) is used, then the spatial resolution achievable can be very high (ca. 10 μm for mm sized components).

The CT image values (grey-levels) provide information on the material X-ray attenuation coefficient at each point in the image. There is considerable current interest in the correction for a number of effects, including especially "beam hardening", which would allow the CT grey levels to be converted to values which are directly proportional to the local material density (Phillips and Lannutti, 1997; Burch 2001a,b).

Cabinet-based systems for real-time radiography contain suitable X-ray sources and detectors for industrial X-ray CT, and can be upgraded to provide a CT capability by addition of a precision turntable and a PC with appropriate image acquisition cards, motor control capabilities and software for image reconstruction and display.

For the work described in this paper, the hardware comprised a 225 kV micro-focus X-ray cabinet system as shown in Fig. 2. This included a detector consisting of a 150 mm image intensifier with a CCD camera generating real-time digital radiography images (1024 \times 1024 pixels resolution, with 12-bit dynamic range). The CT capabilities were provided by a TOMOHAWK CT upgrade system produced by AEA Technology, which included a precision turntable and digital image acquisition card.

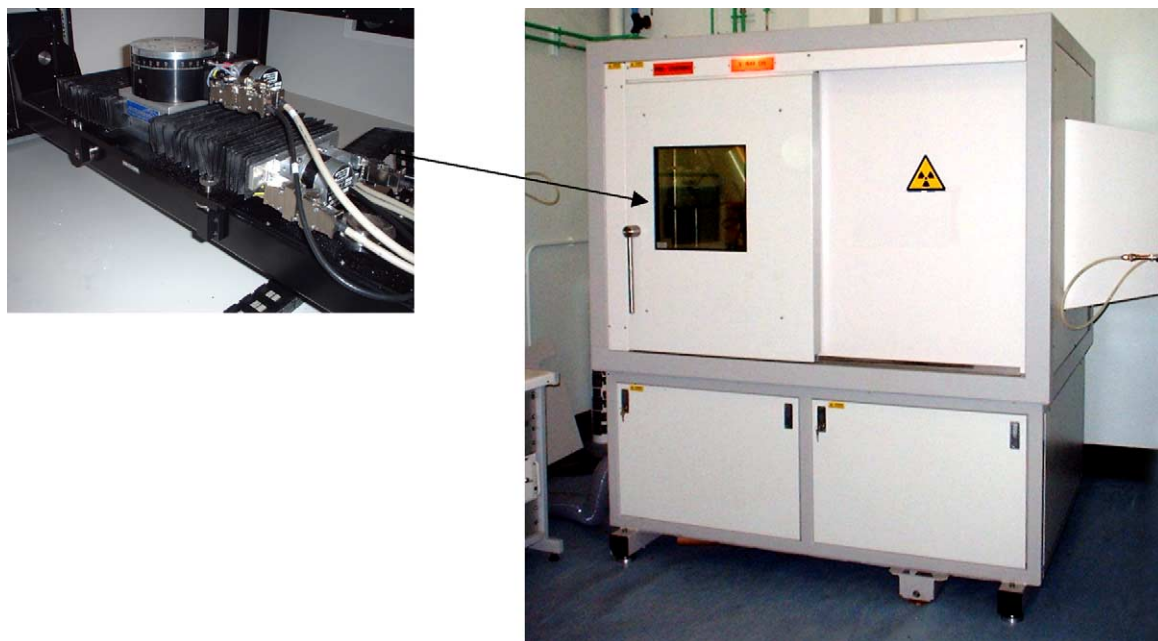


Fig. 2. X-ray CT system.

For the quantitative measurement of density variations within industrial components using X-ray CT, a number of specialised extensions to the standard technique were developed as follows. Firstly, in order to minimise the effects of scattered radiation, collimators were used to limit the spread of the divergent X-ray beam within the X-ray cabinet.

In general, it is also necessary to measure and then correct for the non-linear effects of beam hardening. This correction is necessary because the X-ray source generates radiation having a broad spectrum of photon energies. The dependence of the transmitted X-ray intensity (I) on the linear X-ray attenuation coefficient of the material (μ) is given by

$$I = I_0 e^{-\mu t} \quad (1)$$

where I_0 is the incident X-ray intensity, t is the thickness of material.

As the beam passes through the material, the lower energies are preferentially absorbed since the linear X-ray attenuation coefficient is energy dependent (after Lin and Miller, 2001):

$$\mu = \rho \left(a + \frac{bZ^{3.8}}{E^{3.2}} \right) \quad (2)$$

where ρ is the material density, Z is the material atomic number, E is the photon energy, and a , b are material constants.

The X-ray attenuation was measured for different thicknesses of the material under examination using a set of equi-density calibration discs as described in the following section. This allowed a beam hardening calibration curve to be drawn up. A mathematical function was then fitted to the measured calibration points, which allowed the attenuations from the test object to be “linearised” (Kak, 1979), and hence corrected for beam hardening effects.

Other corrections which are needed to obtain quantitative measurements of material density include:

- Correction using an empty field image. With the X-ray source on, the specimen is removed from the view. The reasons for this correction are that: (a) X-ray detectors are uneven in sensitivity and are often more sensitive towards the centre, and (b) the X-ray beam is also non-uniform, often being stronger in the centre.

- Correction using an image obtained with X-rays off. This correction is necessary because the detector outputs are not necessarily exactly zero for zero X-ray flux.
- “Ring” artefacts, which take the form of weak patterns of concentric circles, are often present on the CT images generated by rotate-only third generation scanning systems. These are caused by coherent detector noise or non-linearities in the detector array. Special techniques for their removal have been developed in the TOMOHAWK CT software.
- Detectors, especially image intensifiers, often have significant spatial distortion which needs to be first measured and then corrected for during CT data acquisition.
- During a CT scan, which can take several minutes, the X-ray flux can vary as a function of time, and hence component rotation angle. These variations need to be monitored and corrected.

3. Materials and tablet preparation

Tablets were manufactured using microcrystalline cellulose (grade Avicel PH102, manufactured by FMC BioPolymer, Cork, Ireland). The nominal mean particle size of the powder is $100\text{ }\mu\text{m}$ and the full density of the material is 1520 kg m^{-3} . The tablets are compressed under controlled conditions. The choice of these conditions is important as they influence the density distribution as described below.

Two capsule shape tablets (Tablets A and B) of identical size but different cup geometries were compressed, as illustrated in Fig. 3a and b. For both tablets the top cup presents a break-line while the bottom cup has the characters “MSD” embossed, Fig. 3c. The characteristics of the tablets and the compaction forces are presented in Table 1.

The die was cleaned prior to compaction. The condition of the die is important because it affects the

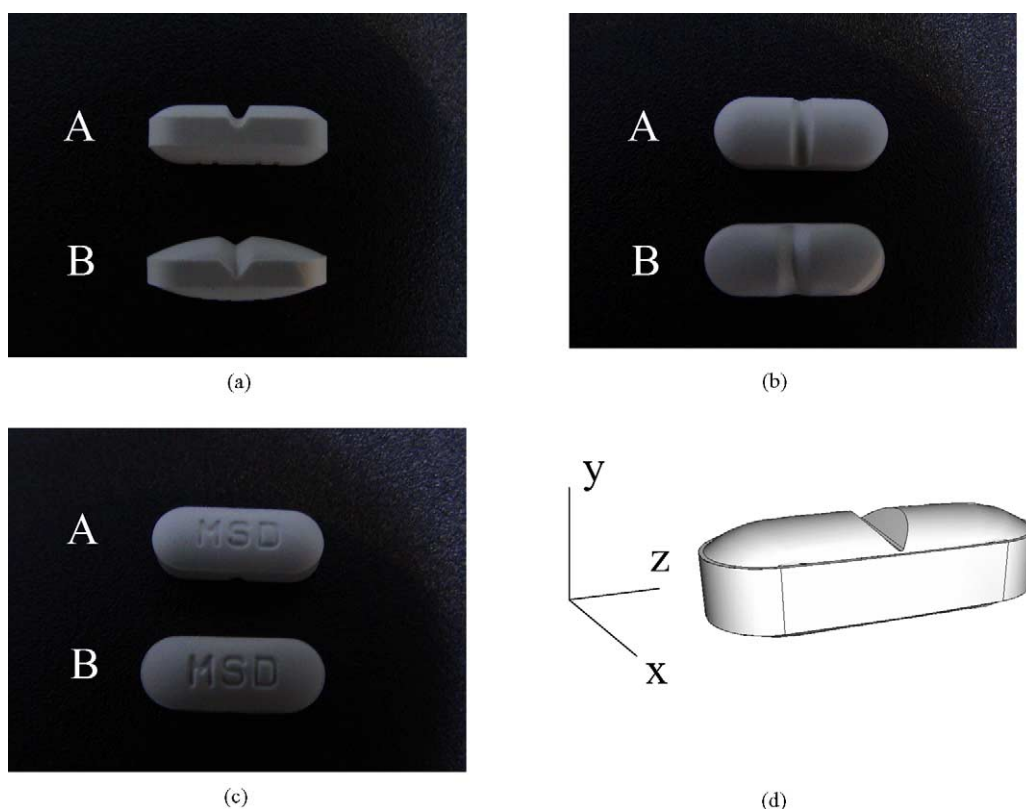


Fig. 3. Tablets.

Table 1
Tablet characteristics

Tablet	Thickness (mm)	Weight (g)	Total volume (mm ³)	Apparent density (kg m ⁻³)	Compaction force (N)
A	3.904	0.190	159.72	1189	4000
B	4.194	0.175	143.25	1221	3500

friction interaction between powder and die during compaction. A clean die results in a high friction coefficient, which impedes the relative sliding of the powder with respect to the die and punches during compaction. This results in particular density distributions; a detailed discussion on such effects for round concave faced tablets is given elsewhere (Sinka et al., 2003).

The powder was fed into the die carefully by hand to achieve a uniform filling because the homogeneity of the filling affects the final density distributions in tablets. Both tablets were compressed in a die such that the bottom punch was maintained stationary with respect to the die.

The choice of the average density in the tablet is also significant. Starting from a uniform state after die filling, the powder aggregate becomes inhomogeneous during compaction. Towards the end of the compaction, when more and more regions of the material achieve near full density, the tablet becomes homogeneous again. Motivated by numerical modelling work on the effect of friction on density inhomogeneity in round flat faced tablets (Sinka et al., 2001), where maximum density inhomogeneity was predicted when the ratio of the average apparent density and the full density of the powder was around 0.8, the target average densities for Tablets A and B were chosen around 1200 kg m⁻³.

In order to generate the data necessary for beam hardening correction, round, flat faced calibration disks were also produced. The requirement for these compacts is that they are uniform. In the absence

of friction between powder and die wall round, flat faced tablets are uniform. Therefore, in order to reduce the effect of friction the dies were pre-lubricated by compressing pure magnesium stearate (a common pharmaceutical lubricant) prior to manufacturing each calibration disk. The characteristics of these tablets are given in Table 2.

4. X-ray CT measurements

For the CT scanning of the tablets described in the section above, it was first necessary to optimise the X-ray and imaging parameters, on the equipment being used. For the present material, which has relatively low density and mean atomic number, Eq. (2) shows that the X-ray attenuation is correspondingly low. Indeed, to obtain adequate contrast on the digital radiographic images, which provide the input to the CT reconstruction algorithm, it was necessary to use the lowest X-ray voltage (40 kV) which gave adequate X-ray flux within the constraints imposed by the detector sensitivity. Improved signal to noise was also achieved by increasing the on-chip integration time on the digital camera to 160 ms.

Measurements of X-ray attenuation were made for increasing numbers of the calibration discs given in Table 2, to quantify the effects of beam hardening for this material and X-ray energy. The results are given in Fig. 4, which shows that the logarithm of I/I_0 was linearly proportional to the mass of calibration tablets in the X-ray beam. As each tablet had closely similar diameters, this shows that for these conditions, any beam hardening was negligible and the linear attenuation coefficient, μ (Eq. (1)) was effectively constant for all material thicknesses. This would not necessarily be the case for larger tablets of the same material, or different materials and/or X-ray energies.

For the CT scanning of Tablets A and B, each was mounted on the precision rotary turntable with their axes vertical, and 3D CT data was then collected for

Table 2
Characteristics of calibration discs

Tablet	Weight (g)	Height (mm)	Diameter (mm)	Density (kg m ⁻³)
CD 1	0.144	1.951	8.756	1225
CD 2	0.143	1.945	8.751	1222
CD 3	0.145	1.969	8.757	1222
CD 4	0.144	1.957	8.754	1222
CD 5	0.143	1.943	8.755	1222
CD 6	0.145	1.972	8.753	1222

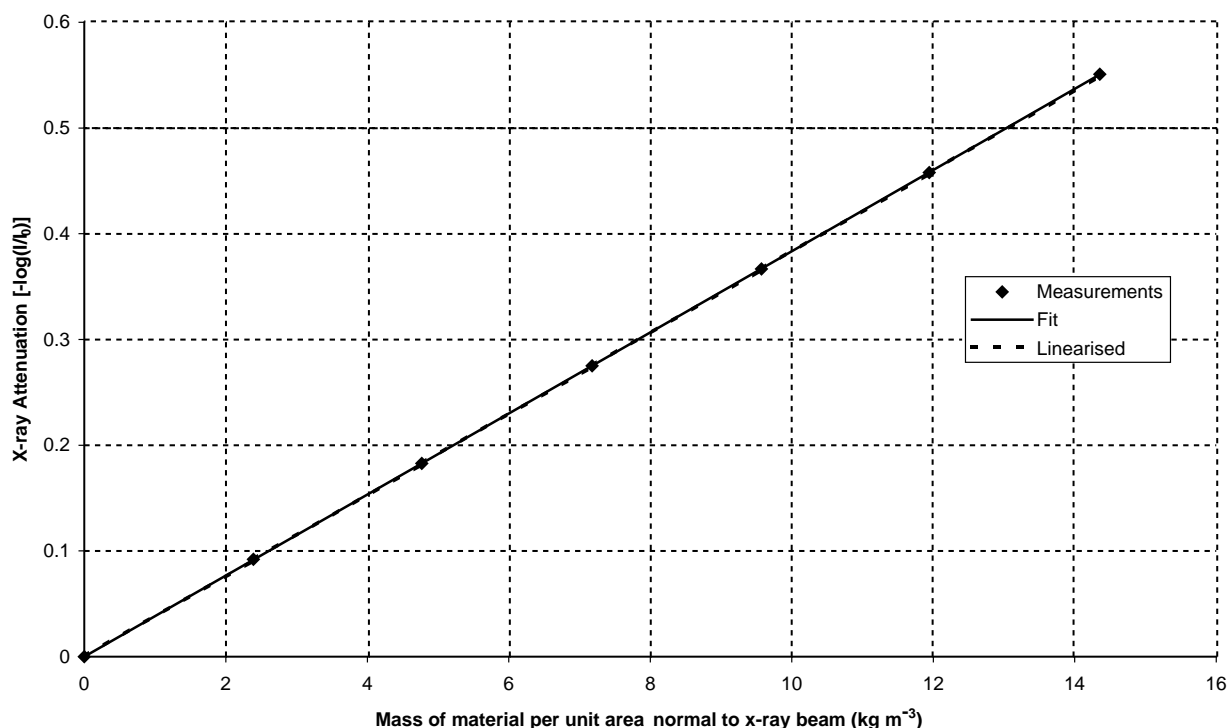


Fig. 4. Correction for beam hardening.

each tablet by rotating $0\text{--}360^\circ$ (CT can be carried out for a half rotation of the specimen, but experience has shown that certain residual instrumental effects can be further minimised by a full rotation through $0\text{--}360^\circ$). The angular increment used in these scans was 0.5° and at each angle 16 radiographic images were averaged to improve signal to noise. Smaller angular increments and greater numbers of image averages would have further improved image quality, but at the expense of longer scan times.

5. Results and discussion

In the following we examine the density distributions in various cross-sections of Tablets A and B. The cross-sections are presented as indicated by the co-ordinate system given in Fig. 3d. For ease of comparison all density maps are prepared using the same colour scale, the labels indicating density in g cm^{-3} .

The vertical $Y\text{--}Z$ cross-sections (along the long axis) at the centres of the tablets are presented

in Fig. 5 and the horizontal $X\text{--}Z$ cross-sections through the mid-height of the tablets are presented in Fig. 6. The left hand edges of the images, where the tablets were mounted on the stage of the TOMOHAWK CT system, are not presented; however, the available data suggest symmetry about the tablet centre line. This is expected as the geometry is symmetrical and the die was filled as uniformly as possible.

Tablet A presents high density regions under the break-line and in the band area—particularly at the edge, as shown in Fig. 5a. The high density region extends around the entire tablet periphery—see Fig. 6a. The density reaches $1200\text{--}1300 \text{ kg m}^{-3}$ locally in some areas. The two very high density spots (around 1400 kg m^{-3}) in Fig. 6a correspond to the positions where the break-line, which is curved around the face of the punch, is at closest with respect to the bottom of the tablet. Other regions, such as the profiles of the characters embossed in the bottom punch or at the top of the tablet next to the break-line present densities of 800 kg m^{-3} or below. The importance of such low

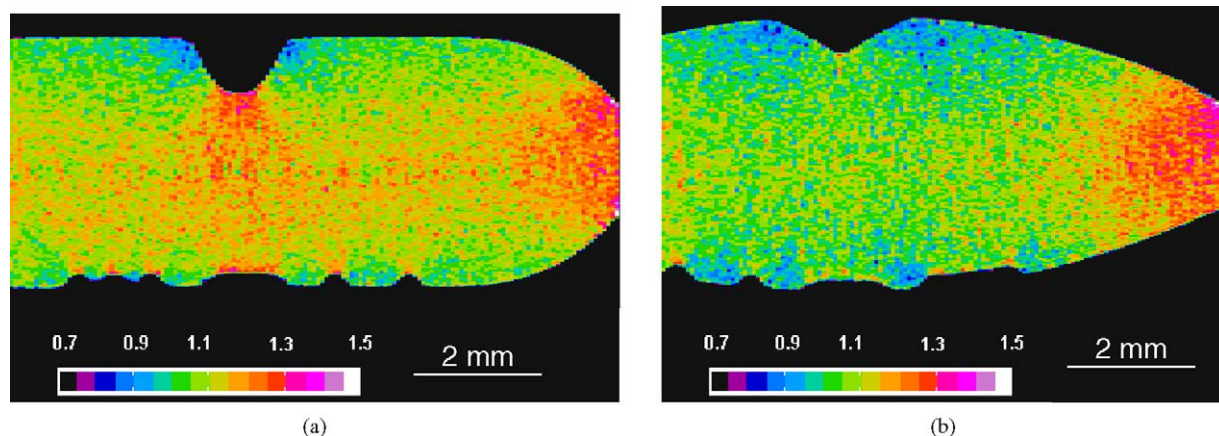


Fig. 5. Density distribution in Y-Z cross-sections.

density regions is that they may affect picking and sticking and are prone to surface erosion, abrasion or breaking during post-compaction operations such as transport, coating or packaging. In addition, the density distribution and associated properties near the break-line may affect the ability to effectively break the tablet in half.

Similar observations can be made for Tablet B as illustrated in Figs. 5b and 6b. The density gradients are amplified due to the particular geometry of the cup. The regions of lower density at the top of the cup (to the sides of the break-line) and at the bottom of

the cup (where the characters are embossed) become more extensive, while the high density areas become more localised. The high density regions around the band area are diminished and there is little evidence of dense regions below the break-line.

Figs. 7 and 8 present X-Y cross-sections (parallel to the break-line) in two positions: next to the break-line and half way between the break-line and the end of the tablet. For Tablet A the sizes of these cross-sections are identical while for Tablet B the cross-section away from the centre is smaller due to the shape of the cup region.

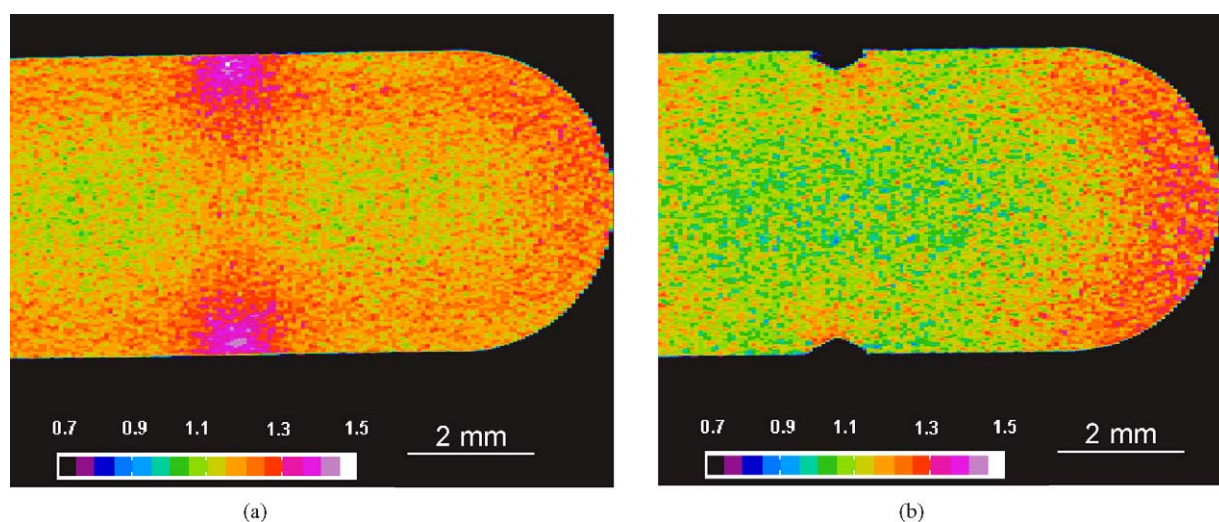


Fig. 6. Density distribution in X-Z cross-sections.

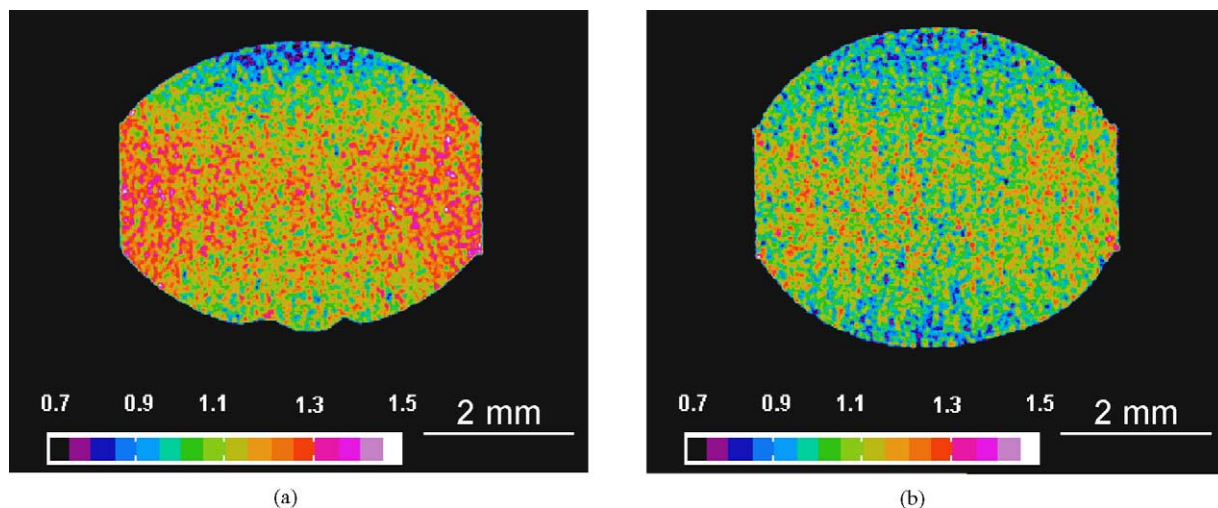


Fig. 7. Density distribution in X–Y cross-sections adjacent to the break-line.

The low density region next to the break-line is illustrated in Fig. 7a for Tablet A, this feature vanishes away from the influence of the break-line (Fig. 8a). The overall density is uniform and the low density regions in the cup area are less intense. The average densities in the whole cross-sections in Figs. 7a and 8a are similar, 1130 and 1140 kg m⁻³, respectively. For Tablet B, however, the average density in the whole cross-section (Fig. 8b) away from the break-line is 1140 kg m⁻³, which is considerably higher than in the

cross-section adjacent to the break-line, 1050 kg m⁻³ (Fig. 7b).

The cross-sections in Figs. 8a and b correspond to positions away from the break-line. It is interesting to observe that for both tablets the density around the band area at the top of the tablet is larger than at the bottom. This effect is brought about by the sequence of punch motions employed: the bottom punch was maintained stationary with respect to the die. The high friction coefficient between powder and die wall re-

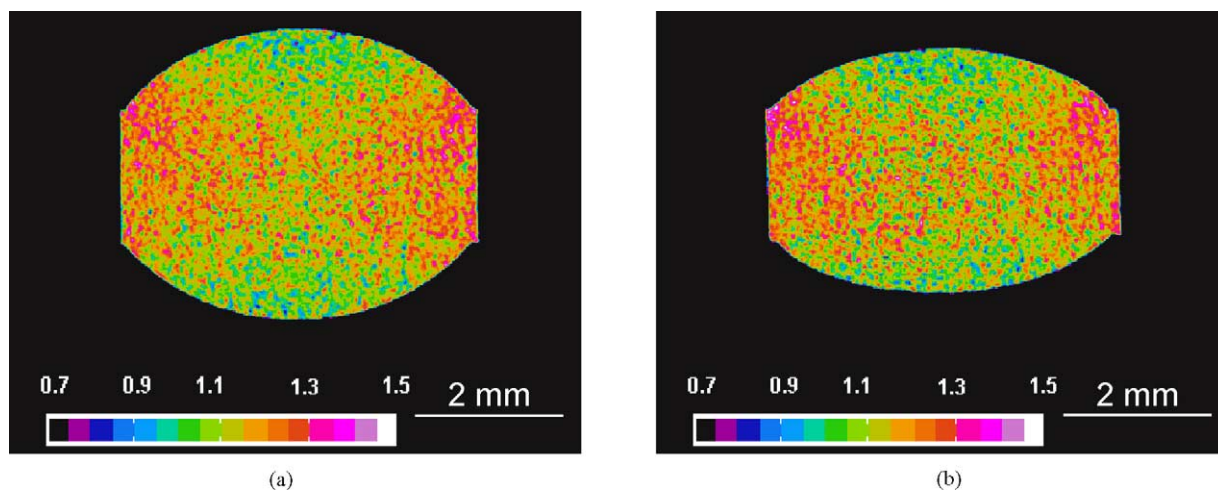


Fig. 8. Density distribution in X–Y cross-sections away from the break-line.

sults in higher density at the top as the top punch is displaced downwards forming the tablet.

The density maps in Fig. 8a and b bear a resemblance to density maps generated using indentation tests for round tablets with concave faces compressed from the same material in previous work (Sinka et al., 2003). In order to understand the origin of such density variations, it is instructive to summarise this discussion. The main factors influencing density distribution in tablets are:

- constitutive behaviour of powder during compaction;
- friction interaction between powder and die wall;
- geometry of die and punches;
- sequence of punch motion;
- initial conditions, which relate to the state of the powder in the die after filling.

We consider the case where the die is cleaned before compaction, when the coefficient of friction between powder and die wall (and powder and punches) is high. As a result there is little or no movement of powder with respect to the punch face as the top punch makes progressive contact with the surface of the powder during compaction. Consequently regions around the band area, where the powder undergoes larger vertical strains, become denser than those in the cup area. Clearly, Tablets A and B present these trends as presented in Fig. 5.

However, the results cannot be generalised. Even for an axisymmetric (round) tablet the powder undergoes complex vertical and radial strain fields during compaction. If the friction coefficient between powder and die wall is reduced (i.e. by pre-lubricating the die wall before compaction), relative sliding of the powder with respect to the punch face is made possible and opposite trends in terms of density maps can be obtained (Sinka et al., 2003), where high density regions develop in the cup and low density is induced in the band region. These conclusions were substantiated by experiments using the surface hardness technique to characterise density and by numerical modelling studies.

The geometry of Tablets A and B is however, not axisymmetric. In this case the 3D density distribution becomes more complicated. The presence of the break-line induces particular effects. Also, the letters embossed on the bottom face of the tablets have a localised effect and the density in these regions is partic-

ularly low. In addition, unlike the bottom punch face which is filled with powder during the die filling, the powder at the top is initially level and thus the powder must flow into the cup region of the upper punch as the initial compaction occurs.

The consequence of low and high density regions is that the local properties of the powders are affected. The strength of a porous material generally increases with density. From this point of view, low density regions may influence adversely the performance of the tablets during post compaction operations such as coating (i.e. low density regions may erode), packaging, transport and use. In addition, the localised disintegration and dissolution may be affected.

6. Conclusions

This work illustrates that X-ray microtomography can be applied successfully to examine density variation in low density porous materials such as pharmaceutical tablets. These compacts give low X-ray attenuation, therefore non-linear experimental effects, such as beam hardening and scattering of the X-ray radiation have small effects. However, quantitative density maps require correction for all factors described above.

Quantitative density maps were produced in various cross-sections of model tablets, which were engineered to present large density variations. Given that the full density of the material is 1500 kg m^{-3} , the presence of regions having a density of 800 kg m^{-3} or below, with other regions of 1400 kg m^{-3} or higher density, indicates considerable inhomogeneity. Tablet compaction is a complex process and all contributing factors discussed above have an inter-dependent influence in determining the microstructure of a tablet. We stress that density maps such as those obtained in this work should not be generalised and each situation should be assessed individually. The use of non-destructive X-ray microtomography allows one to characterise the density distribution of an individual tablet and then further characterise the mechanical and/or dissolution behaviour. Comprehensive characterisation of the material response during compaction and the friction behaviour together with detailed analysis of compaction can aid formulation design, process development and tablet image design.

Acknowledgements

Support from the Department of Trade and Industry (UK) through the programme “Minimising Density Variations in Powder Compacts—MPM5.2” is acknowledged. The Manchester Materials Science Centre is thanked for the provision of X-ray Facilities. I.C.S. and J.C.C. wish to thank the management of PR&D, Merck Research Laboratories, particularly Drs. D.E. Storey and S.D. Reynolds, for their support.

References

- Burch, S.F., 2001a. Measurement of density variations in compacted parts using X-ray computed tomography. In: *Proceedings of EuroPM2001*, Nice, France, October 22–24, pp. 398–404.
- Burch, S.F., 2001b. X-ray computerised tomography for quantitative measurement of density variations in materials. *Insight* 43, 29–31.
- Farber, L., Tardos, G., Michaels, J.N., 2003. Use of X-ray tomography to study the porosity and morphology of granules. *Powder Technol.* 132, 57–63.
- Kak, A.C., 1979. Computerized tomography with X-ray, emission and ultrasound sources. *Proc. IEEE* 67, 1245–1272.
- Kong, C.M., Lannutti, J.J., 2000. Localised densification during the compaction of alumina granules: the stage I–II transition. *J. Am. Ceram. Soc.* 83, 685–690.
- Lannutti, J.J., 1997. Characterisation and control of compact microstructure. *MRS Bull.* 22, 38–44.
- Li, W., Nam, J., Lannutti, J.J., 2002. Density gradients formed during compaction of bronze powders: the origins of part-to-part variations. *Metall. Mater. Trans. A* 33A, 165–170.
- Lin, C.L., Miller, J.D., 2000. Pore structure and network analysis of filter cake. *Chem. Eng. J.* 80, 221–231.
- Lin, C.L., Miller, J.D., 2001. A new cone beam X-ray microtomography facility for 3D analysis of multiphase materials. In: *Proceedings of 2nd World Congress on Industrial Process Tomography*, Hannover, Germany, August 29–31.
- Macleod, H.M., Marshall, K., 1977. The determination of density distributions in ceramic compacts using autoradiography. *Powder Technol.* 16, 107–122.
- Mersereau, R.M., 1974. Digital reconstruction of multidimensional signals from their projections. *Proc. IEEE* 62, 1319–1338.
- Nielsen, S.F., Poulsen, H.F., Beckmann, F., Thorning, C., Wert, J.A., 2003. Measurements of plastic displacement gradient components in three dimensions using marker particles and synchrotron X-ray absorption microtomography. *Acta Materialia* 51, 2407–2415.
- Phillips, D.H., Lannutti, J.J., 1997. Measuring physical density with X-ray computed tomography. *NDT&E Int.* 30, 339–350.
- Sinka, I.C., Cunningham, J.C., Zavaliangos, A., 2001. Experimental characterization and numerical simulation of die wall friction in pharmaceutical powder compaction. In: *Proceedings of PM2TEC 2001 International Conference on Powder Metallurgy & Particulate Materials*, Part 1, New Orleans, LA, USA, 13–17 May, pp. 46–60.
- Sinka, I.C., Cunningham, J.C., Zavaliangos, A., 2002. Density distributions in pharmaceutical tablets: experiments and modelling. In: *Proceedings of 2002 International Conference on Process Modelling in Powder Metallurgy & Particulate Materials*, Newport Beach, CA, USA, October 28–29. Compiled by Lawley, A., Smith, L., Smudgeresky, J.E., Published by Metal Powder Industries Federation, Princeton, NJ, USA, pp. 123–132.
- Sinka, I.C., Cunningham, J.C., Zavaliangos, A., 2003. The effect of wall friction in the compaction of pharmaceutical tablets with curved faces: a validation study of the Drucker–Prager Cap model. *Powder Technol.* 133, 33–43.
- Train, D., 1957. Transmission of forces through a powder mass during the process of pelleting. *Trans. Inst. Chem. Eng.* 35, 258–266.